Animal Nutrition 9 (2022) 84–99

Contents lists available at ScienceDirect

Animal Nutrition

journal homepage: http://www.keaipublishing.com/en/journals/aninu/

Original Research Article

Multi-omics analysis reveals gut microbiota-induced intramuscular fat deposition via regulating expression of lipogenesis-associated genes

Chunlin Xie [a, b, c, d], Junyong Teng [a, b, c, d], Xinkai Wang [a, b, c, d], Baoyang Xu [a, b, c, d], Yaorong Niu [a, b, c, d], Libao Ma [a, b, c, d], Xianghua Yan [a, b, c, d, *]

[a] State Key Laboratory of Agricultural Microbiology, College of Animal Sciences and Technology, Huazhong Agricultural University, Wuhan, Hubei, 430070, China
[b] Hubei Hongshan Laboratory, Wuhan, Hubei, 430070, China
[c] The Cooperative Innovation Center of Sustainable Pig Production, Wuhan, Hubei, 430070, China
[d] Hubei Provincial Engineering Laboratory for Pig Precision Feeding and Feed Safety Technology, Wuhan, Hubei, 430070, China

ARTICLE INFO

Article history:
Received 25 July 2021
Received in revised form
14 October 2021
Accepted 20 October 2021
Available online 7 December 2021

Keywords:
Gut microbiota
Lipid deposition
Intramuscular fat
Meat quality
Fecal microbiota transplantation

ABSTRACT

The gut microbiome has great effects on the digestion, absorption, and metabolism of lipids. However, the microbiota composition that can alter the fat deposition and the meat quality of pigs remains unclear. Here, we used Laiwu (LW) pigs (a native Chinese breed with higher intramuscular fat) compared with commercial crossbreed Duroc × (Landrace × Yorkshire) (DLY) pigs to investigate the effects of microbiota on meat quality, especially in intramuscular fat content. A total of 32 DLY piglets were randomly allotted to 4 groups and transplanted with fecal microbiota from healthy LW pigs. The results indicated that the high dose of fecal microbiota transplantation (HFMT) selectively enhanced fat deposition in longissimus dorsi ($P < 0.05$) but decreased backfat thickness ($P < 0.05$) compared with control group. HFMT significantly altered meat color and increased feed conversation ratio ($P < 0.05$). Furthermore, the multi-omics analysis revealed that *Bacteroides uniformis*, *Sphaerochaeta globosa*, *Hydrogenoanaerobacterium saccharovorans*, and *Pyramidobacter piscolens* are the core species which can regulate lipid deposition. A total of 140 male SPF C57BL/6j mice were randomly allotted into 7 groups and administrated with these 4 microbes alone or consortium to validate the relationships between microbiota and lipid deposition. Inoculating the bacterial consortium into mice increased intramuscular fat content ($P < 0.05$) compared with control mice. Increased expressions of lipogenesis-associated genes including cluster of differentiation 36 (*Cd36*), diacylglycerol O-acyltransferase 2 (*Dgat2*), and fatty acid synthase (*FASN*) were observed in skeletal muscle in the mice with mixed bacteria compared with control mice. Together, our results suggest that the gut microbiota may play an important role in regulating the lipid deposition in the muscle of pigs and mice.

1. Introduction

The mammalian gut microbial community plays a pivotal role in host health, including nutrients metabolism, immunity, and disease (Claesson et al., 2012; Desai et al., 2016). Numerous exploratory studies have characterized the contribution of microbiota on host health and indicated marked shifts in the relative abundance of various phyla or species in various physiological statuses (Franzosa et al., 2019; Li et al., 2017, 2020a). For instance, comparisons of the gut microbiota of lean and obese people indicated that the relative abundance of Bacteroidetes and Firmicutes are associated with obesity, and a significantly greater increase in total body fat was observed in 'obese microbiota' recipient mice than in 'lean microbiota' recipient mice (Ley et al., 2005, 2006; Turnbaugh et al., 2006). Clearly, the individual-specific microbial composition is stable over time in the mature mammalian intestine (Fassarella et al., 2020). A

* Corresponding author.
E-mail address: xhyan@mail.hzau.edu.cn (X. Yan).
Peer review under responsibility of Chinese Association of Animal Science and Veterinary Medicine.

Production and Hosting by Elsevier on behalf of KeAi

https://doi.org/10.1016/j.aninu.2021.10.010

recent study has indicated that the reconstitution of the donor-specific microbial community via fecal microbiota transplantation (FMT) is possible by transferring the partly metabolic phenotype from the donor to the recipient (Fabbiano et al., 2018). Thus, the earlier intervention of mammalian gut microbial composition is a possible strategy to modulate host functions.

Global meat consumption is rising and likely to continue in the future (Godfray et al., 2018). The influence of factors like price and income is likely to decline over time, so that meat quality will become an important factor in consumer choice. Growing evidence makes it clear that specific probiotic supplementation is efficient in ameliorating animal health and improving meat quality. For example, dietary inclusion of *Clostridium butyricum* and *Rhodobacter capsulatus* have been suggested to improve meat quality and fatty acid profile in the broiler (Salma et al., 2007; Yang et al., 2010). It has also been reported that direct-fed probiotics can improve growth performance and feed efficiency in pigs (Kyriakis et al., 1999). Lipid contents in farm animals, especially intramuscular fat (IMF) content, is one of the most important traits which have a direct impact on the aroma and tenderness of meat (Crespo-Piazuelo et al., 2020). Intramuscular fat determines the oxidative stability and the textural properties of muscle, which are positively correlated with meat flavor, tenderness, juiciness, and overall liking (Wood et al., 2008). However, the main object of breeding strategies in cosmopolitan pig breeds has been to increase lean meat percentage and growth efficiency, which has resulted in a reduction of IMF content and compromised meat quality (Lonergan et al., 2001). A previous study indicated that it is possible to regulate the IMF and backfat deposition by dietary lysine restriction during the finisher period of Duroc × (Landrace × Yorkshire) (DLY) pigs (Suarez-Belloch et al., 2015). Given the evidence that the IMF can be increased with no significant effect on backfat thickness after feeding low protein diets in pigs (Doran et al., 2006; Wood et al., 2004), it is plausible to modulate fat deposition via nutritional manipulation. However, the use of microbiota on improving IMF content in pigs was rarely reported. Metabolites and proteins reside at the critical interface of the microbiome and the host lipid metabolism. To study the complex biological process holistically, a few studies have combined multi-omics data to highlight the interrelationships of the revolved biomolecules and their functions (Dyar et al., 2018; Li et al., 2020b; Mars et al., 2020). Here, we integrate multi-omics analysis to provide specific insight into the relationship between microbiota and fat deposition.

The Laiwu (LW) pig is a native Chinese breed characterized by its high IMF content and excellent meat quality (Huang et al., 2018). However, other commercial breeds such as Landrace, Duroc, Yorkshire, and DLY are widely used because of faster growth rates and an increase in the lean-to-fat ratio, ignoring IMF content and meat quality (Chen et al., 2017; Choi et al., 2014; Rusc et al., 2011; Wu et al., 2013). Based on the studies outlined above, we hypothesized that utilizing the specific gut microbial community in LW pigs might provide a potential strategy to improve the meat quality of commercial pigs. Therefore, the FMT was performed from LW pigs to DLY pigs aiming to evaluate the effect of gut microbiota on IMF content and pork quality.

2. Materials and methods

2.1. Animal ethics

The experimental protocols of this study were approved by the Institutional Animal Care and Use Committee of Huazhong Agricultural University, Wuhan, China (approval numbers: HZAUSW-2019-012, HZAUMO-2019-042). A total of 32 DLY pigs and 140 C57BL/6j mice were given free access to water and feed.

2.2. Stool sample connection and fecal suspension preparation

Fifty healthy LW pigs with similar body weights (80 kg) were randomly selected and fresh feces were collected from these pigs. The fresh fecal samples were diluted and homogenized in sterile saline containing 10% glycerol and then passed through steel tea strainers (sterilized) followed by a 0.224-mm stainless cell strainer to remove particles as previously describes (Hamilton et al., 2012). The suspension was dispensed to cryotubes and stored in liquid nitrogen until used for FMT. Part of the fresh feces was collected and stored in liquid N_2 for 16S rDNA sequencing.

2.3. Fecal microbiota transfer experiments

Stool samples from LW pigs were selected and prepared as described and inoculated into DLY pigs via oral gavage. A total of 32 age-matched crossbred pigs (DLY) with an average body weight of 30 kg were randomly assigned to 4 treatment groups and then divided into 16 pens (2 pigs per pen). The basal diets composition is shown in Table S1. The pigs received 5 mL sterile saline (control group, Ctrl), sterile FMT (SFMT group), low dose of FMT (LFMT group, 10^7 CFU/mL), and high dose of FMT (HFMT group, 10^8 CFU/mL) by oral gavage once every other day until 90 kg. All the pigs had unlimited access to feed and water during the experimental period. The diarrheal pigs were recorded during the first 30 d of FMT. The body weights of pigs were measured every month and the feed intake of each pen was recorded. At d 90, pigs were fasted for 12 h and slaughtered by neck bleeding after electric shock. Fresh feces were collected from the rectum and stored at −80 °C for microbiota analysis. Segments of the small intestine (duodenum, jejunum, and ileum) were taken and fixed in 4% paraformaldehyde for histological analysis. The longissimus dorsi muscle (500 g) was removed for meat quality determination immediately. Part of longissimus dorsi and small intestine tissues were excised and immediately stored in liquid N_2 for metabolic and proteomic analysis.

2.4. Mouse intervention study with microbes

Bacteroides uniformis (DSM 6597^T), *Sphaerochaeta globosa* (DSM 22777^T), *Hydrogenoanaerobacterium saccharovorans* (DSM 24774^T), and *Pyramidobacter piscolens* (DSM 21147^T) were purchased from the DSMZ and cultured according to the manufacturer's instructions. Strains were stored in 10% glycerol at −80 °C until use. Cohorts of male SPF C57BL/6j mice with similar weights (11.4 ± 0.02 g) were weaned at 28 d of age and randomly divided into 7 groups. The antibiotic cocktail dissolved in mouse drinking water has previously been shown to suppress commercial gut microbiota, and included 50 μg/mL streptomycin, 100 μg/mL neomycin, 100 U/mL penicillin, 100 μg/mL metronidazole, 50 μg/mL vancomycin, 100 μg/mL ceftazidime, 125 μg/mL ciprofloxacin, 1 mg/mL bacitracin, and 170 μg/mL gentamycin (Chevalier et al., 2015). We treated mice with a cocktail of antibiotics for 1 week before the microbiota gavage experiment. Thereafter, the mice underwent oral gavage with sterile PBS (Ctrl group, and short-chain fatty acids [SCFA] group), suspension (200 mL, 10^8 CFU/mL) containing *B. uniformis* (B.uni group), *S. globosa* (S.glo group), *H. saccharovorans* (H.sac group), and *P. piscolens* (P. pis group) respectively, for 4 weeks. In addition, the mice in the SCFA group were given a mixture of 67.5 mmol/L sodium acetate, 40 mmol/L sodium butyrate, and 25.9 mmol/L sodium propionate dissolved in drinking

water as previously described (Lahiri et al., 2019). The mice in the Mix group were administrated with a mixed bacterial suspension (200 mL, 10^8 CFU/mL), containing *B. uniformis*, *S. globosa*, *H. saccharovorans*, and *P. piscolens*, by gastric gavage every other day for 4 weeks. Mice were allowed free access to sterile water and feed and the fresh sterile water was changed every day. At the end of the experiment, mice were fasted overnight and euthanized, and soleus, tibialis anterior (TA), extensor digitorum longus (EDL), gastrocnemius, and quadriceps were weighed and collected for qPCR analysis. The IMF of gastrocnemius was measured with an Elisa kit (jlc − A10563).

2.5. Microbial genomic DNA extraction, amplicon generation, and sequencing

Genomic DNA was isolated from stool samples (stored at −80 °C) using the combined method of cetyl trimethyl ammonium bromide (CTAB) and bead-beating as previously described (Hu et al., 2016). The V4 region of the 16S rDNA was amplified by PCR with primers as F: 5′-NNNNNNNNGTGTGCCAGCMGCCGCGGTAA-3′ and R: 5′-GGACTACHVGGGTWTCTAAT-3′. Thereafter, the amplicons were quantified and sequenced pair end on the Illumina MiSeq platform. All 16S rDNA sequencing data were publicly available in the National Center for Biotechnology Information (NCBI) Sequence Read Archive and are accessible under BioProject accession number PRJNA683194.

2.6. Sequencing data analysis

Sequencing data were filtered and merged to tags with the Connecting Overlapped Pair-End (COPE) software (v1.2.1) (Liu et al., 2012). The tags were clustered to OUT at 97% sequence similarity. Mothur (v1.31.2) software was used to classify the bacterial OUT representative sequences based on Ribosomal Database Project (RDP) database. The weighted UniFrac analysis was used to measure the β-diversity of the microbiome and analyzed with the Quantitative Insights Into Microbial Ecology (QIIME, v1.80) software package. The PCoA and clustering heat map were drawn with R (v3.3.3) programming language based on weighted UniFrac diversity distance. Significant differences in relative abundance between the groups were determined by Metastats software. The Linear discriminant analysis Effect Size (LEfSe) analysis was performed by LEfSe software. The Bray–Curtis distance was done using the vegdist (method = "bray") function of a vegan package in R (v3.3.3) and shown by the PCA analysis.

2.7. Histological analysis

To perform histology analysis, the small intestinal segments (duodenum, jejunum, and ileum) were removed and gently flushed with PBS, fixed in 4% paraformaldehyde. Subsequently, the intestine was swiss rolled and embedded in paraffin. These segments were sectioned at 5 μm and stained with hematoxylin and eosin (H&E). Images of the intestine were obtained with a light microscope at 40× and 100× magnification. The villi heights and crypts depths were measured with Image-Pro Plus software.

2.8. Measurement of fecal SCFA

Feces stored at −80 °C were used to quantify fecal SCFA in pigs. The concentration of SCFA was determined using gas chromatography (Zhernakova et al., 2016). Briefly, 0.2 g feces were mixed with Milli-Q water (100 μL per 100 mg of material) and extracted by vortexing for 5 min. The pooled extraction was centrifuged at 12,000 × *g* for at least 3 min. The supernatant (0.2 mL) was mixed with 40 μL metaphosphoric acid to extract liposoluble components. The samples were then centrifuged (12,000 × *g* for 15 min, 4 °C) after overnight at 4 °C. The supernatants (1 mL each) were pipetted and filtered through a 0.22-μm filter and then injected to Trace GC 1,300. The temperature of injector and flame ionization detector were 150 and 250 °C, while the oven temperature was 140 °C.

2.9. Measurement of meat quality traits

At the end of the feeding trial, all pigs were individually weighed and slaughtered to analyze meat quality. The longissimus dorsi muscles (on the right side of the carcass) were removed and used to measure meat quality traits. Marbling score was calculated according to National Pork Producers Council (NPPC) guidelines. Meat color was measured after exposure to the air at room temperature for 30 min with a colorimeter (Minolta CR-400; Konica Minolta, Tokyo, Japan). The pH values were measured at approximately 45 min and 24 h after slaughter with a digital pH meter. Drip loss was measured by cutting meat samples into 15 mm × 15 mm × 30 mm and storage at 4 °C for 48 h, calculating the initial and final weight. The shear force was measured by cooking samples to a final core temperature of 75 °C, then removing a 1-cm round strip for Warner-Bratzler shear force (Model 2356X; Salter Brecknell, Manhattan, KS, USA) test. The contents of water, protein, and IMF in longissimus dorsi were analyzed with near-infrared spectroscopy (Aquila Blue, Germany) as described previously (Lambe et al., 2021). In addition, longissimus dorsi muscles from LW pigs (90 to 120 kg) were collected to measure IMF by Near-infrared spectroscopy.

2.10. Untargeted metabolomics profiling

2.10.1. Sample preparation

Muscular metabolites were extracted by mixing thawed tissue (25 mg) and chilled methanol-water (1:1, 800 μL) solution, ground with TissueLyser and placed at −20 °C for 2 h. Samples were then centrifuged at 30,000 × *g* (4 °C for 15 min) and 650 μL was transferred to a new tube. Each sample was centrifuged at 25,000 × *g* (4 °C for 20 min), and 550 μL supernatant was transferred to a clean tube. Next, 1 mL mixture of acetonitrile, methanol, and acetone (8:1:1) was taken to precipitate the proteins, and 400 μL supernatant was transferred to the equilibrated and activated solid-phase extraction (SPE) column after centrifugation. The supernatant was discarded after two rounds of centrifugation, reconstituted in 400 μL of 100% acetonitrile, then eluted solution was transferred into a clean tube for metabolic analysis.

2.10.2. Metabolomics analysis

Liquid chromatographic separations were achieved on an ACQUITY UPLC HSS T3 column (100 mm × 2.1 mm, 1.8 μm, Waters, UK) using an ultra-performance liquid chromatography (UPLC) system (Waters, UK), and MS was performed on a high-resolution tandem mass spectrometer Xevo G2 XS QTOF (Waters, UK). The Q-TOF was run in both positive and negative ion modes. The mobile phase was composed of buffers: (A) water with 0.1% formic acid and (B) acetonitrile with 0.1% formic acid. The follow rate was set at 0.4 mL/min with the following gradient elution conditions: 0 to 2 min, 100% buffer A; 2 to 11 min, 0 to 100% buffer B; 11 to 13 min, 100% buffer B; 13 to 15 min, 0 to 100% buffer A. The data of the mass spectrometer were acquired in Centroid MSE mode. The alignment, extraction, normalization, deconvolution, and compound identification of peak were monitored by Progenesis QI software (v 2.2). Furthermore, QC samples were acquired to evaluate the stability of LC–MS at acquisition. The local polynomial regression fitting signal

correction which was performed on the real sample signal was based on QC sample information (Dunn et al., 2011).

2.11. Proteomics analysis

Quantitative proteomics iTRAQ was conducted to determine the protein profile of the small intestine and muscle. The samples were mixed with lysis buffer (8 mol/L urea, 10 mmol/L dithiothreitol, 4% CHAPS (3-[(3-cholamidopropyl)dimethylammonio]-1-propanesulfonate), 40 mmol/L Tris-HCl, 1 mmol/L PMSF (phenylmethanesulfonyl fluoride), 2 mmol/L EDTA, pH 8.5) and sonicated with TissueLyser (50 Hz, 2 min) to release proteins. The supernatant was transferred into a clean EP tube after centrifugation (25,000 × *g*, 4 °C for 20 min). To reduce the proteins, 10 mmol/L dithiothreitol was added at 56 °C for 1 h, then the supernatant was alkylated with 55 mmol/L iodoacetamide for 45 min in dark conditions. Samples were centrifugated at 25,000 × *g* (4 °C for 20 min), the supernatants were transferred to a clean polyethylene (PE) tub, the protein concentration was quantified by Bradford assay. The quality of protein extraction was measured with SDS-PAGE. Approximately 100 μg protein solution was diluted with 100 mmol/L TEAB (tetraethylammonium bromide) for 4 times and digested with Trypsin Gold (trypsin-to-protein ratio = 40:1) at 37 °C for 16 h. The peptides were desalted using Strata X C18 column (Phenomenex) after digestion and dried by vacuum centrifugation. To dissolve peptides, 30 μL TEAB (0.5 mol/L) was added. The samples were combined and labeled with iTRAQ reagents according to the manufacturer's protocol. The separation of labeled peptides was performed on a high pH RP column using the Shimadzu LC-20AB HPLC Pump system. The labeled samples were reconstituted in 2 mL buffer B (95% H_2O and 5% ACN, pH 9.8) and injected into a column (5 μm particles). The peptides were eluted at the flow rate: 1 mL/min for 10 min with a gradient of 5% buffer B, 5% to 35% buffer B for 40 min, 35% to 95% buffer B for 1 min, and then maintained in 95% buffer B for 3 min, decreased to 5% within 1 min, and equilibrated with 5% buffer B for 10 min. The peptides elution was collected every 1 min and pooled as 20 fractions following being vacuum dried.

2.11.1. LC–MS/MS analysis

The LC–MS/MS analysis was performed with Thermo Scientific UltiMate 3000 UHPLC system. The fractions were resuspended with buffer A (0.1% formic acid, 2% acetonitrile) and centrifuged with 20,000 × *g* for 10 min, then 5 μL supernatant was loaded onto a trap and an analytical column at 5 μL/min for 8 min, then eluted onto a homemade nanocapillary C18 column (inner diameter 75 μm × 25 cm). The gradient run was set: 300 nL/min for 40 min in 5% to 25% buffer B, linear gradient to 80% buffer B for 2 min, then maintained at 80% buffer B for 2 min, finally returned to 5% buffer B in 1 min and equilibrated for 6 min. The separated peptides were analyzed with tandem mass spectrometry using Q EXACTIVE HF X (Thermo Fisher Scientific, San Jose, CA) system combined with online to the HPLC.

2.11.2. Bioinformatics pipeline for data analysis

Quantitation and analysis of labeled peptides were performed by automated IQuant software (Wen et al., 2014). The data were filtered based on a PSM-concentration and false discovery rate (FDR) at 1% to reduce false positive results as previously described (Savitski et al., 2015). The identified peptide sequence contains at least 1 unique peptide. The differentially expressed proteins were identified by fold change >1.5 or <0.5 (mean value of all groups), $P < 0.05$ (*t*-test of all groups). The functional variation analysis and details of the lipid metabolism pathway were performed using the Kyoto Encyclopedia of Genes and Genomes (KEGG) database. The Ingenuity Pathway Analysis (IPA) software (www.ingenuity.com) was used to study functional characteristics and analyze interaction networks. The LC–MS raw data have been deposited to the ProteomeXchange Consortium via the PRoteomics IDEntifications (PRIDE) database partner repository with the dataset identifier PXD023197.

2.12. qPCR for target genes

Total RNA was extracted from the muscle of mice. The relative expression of genes associated with lipogenesis was measured by qPCR. Oligonucleotide primers were used to amplify target genes are shown in Table S2. The quantitative polymerase chain reaction (PCR) program consisted of an initial denaturation at 95 °C (10 min) followed by 40 cycles of denaturation at 95 °C for 15 s, 60 °C for 30 s, 72 °C for 30 s, annealing at 60 °C for 30 s and extension at 72 °C for 30 s.

2.13. Statistical analysis

The sample size for each group was chosen based on study feasibility and all quantitative assays were performed using at least three technical replicates unless specifically stated otherwise. We performed unpaired two-tailed Student's *t*-test or one-way analysis of variance ANOVA followed by Tukey's multiple comparison's test to analyze the influence of treatments. The detailed descriptions of the statistical methods are shown in each the legends of each Figure. $P < 0.05$ was considered statistically significant ($^*P < 0.05$, $^{**}P < 0.01$, $^{***}P < 0.001$). The data are shown as mean ± SEM and produced by GraphPad Prism 7 software.

3. Results

3.1. Distinct microbiome and higher IMF content in Laiwu pigs

The IMF content is an important trait strongly correlated with the sensory properties of meat. Previous studies have detected the IMF content of different commercial pig breeds including Yorkshire, 1.54% ($n = 12$); Landrace, 1.79% ($n = 60$); Duroc, 2.98 ($n = 200$); and DLY, 2.21% ($n = 132$) (Chen et al., 2017; Choi et al., 2014; Rusc et al., 2011; Wu et al., 2013). To confirm the IMF content in LW pigs, longissimus dorsi muscles were collected from 28 LW pigs at the market weight, and then the IMF content was measured using Near-infrared spectroscopy. As expected, the IMF in LW pigs was (10.78 ± 0.26)% (mean ± SEM), remarkably higher than that in commercial pig breeds (Table S3). To investigate the characteristics of the microbial composition between DLY and LW pigs, the feces were collected and analyzed through 16S rDNA sequencing. Principle component analysis (PCA) comparing bacterial diversity within individual subjects revealed that LW pigs harbored a distinct bacterial community compared to DLY pigs (Fig. 1A). The heatmap of cluster analysis revealed a higher similarity of all genera among different samples within-group (Fig. 1B). Furthermore, comparative analysis of microbial composition at phylum and genus levels between LW and DLY pigs was performed based on metastats analysis (Tables S4 and 5). At phylum level, Firmicutes was most dominated in DLY pigs and Bacteroidetes was significantly higher in LW pigs. The relative abundance of Proteobacteria was significantly higher in DLY pigs. Conversely, Elusimicrobia showed a higher abundance in LW pigs (Fig. 1C). At genus level, *Oscillospira* was the most abundant among significantly higher bacteria in DLY pigs followed by Escherichia. On the other hand, *Phascolarctobacterium*, *Parabacteroides*, *Bacteroides*, *Anaeroplasma*, *Sphaerochaeta*, and *Akkermansia* showed higher relative abundance in LW pigs (Fig. 1C). The

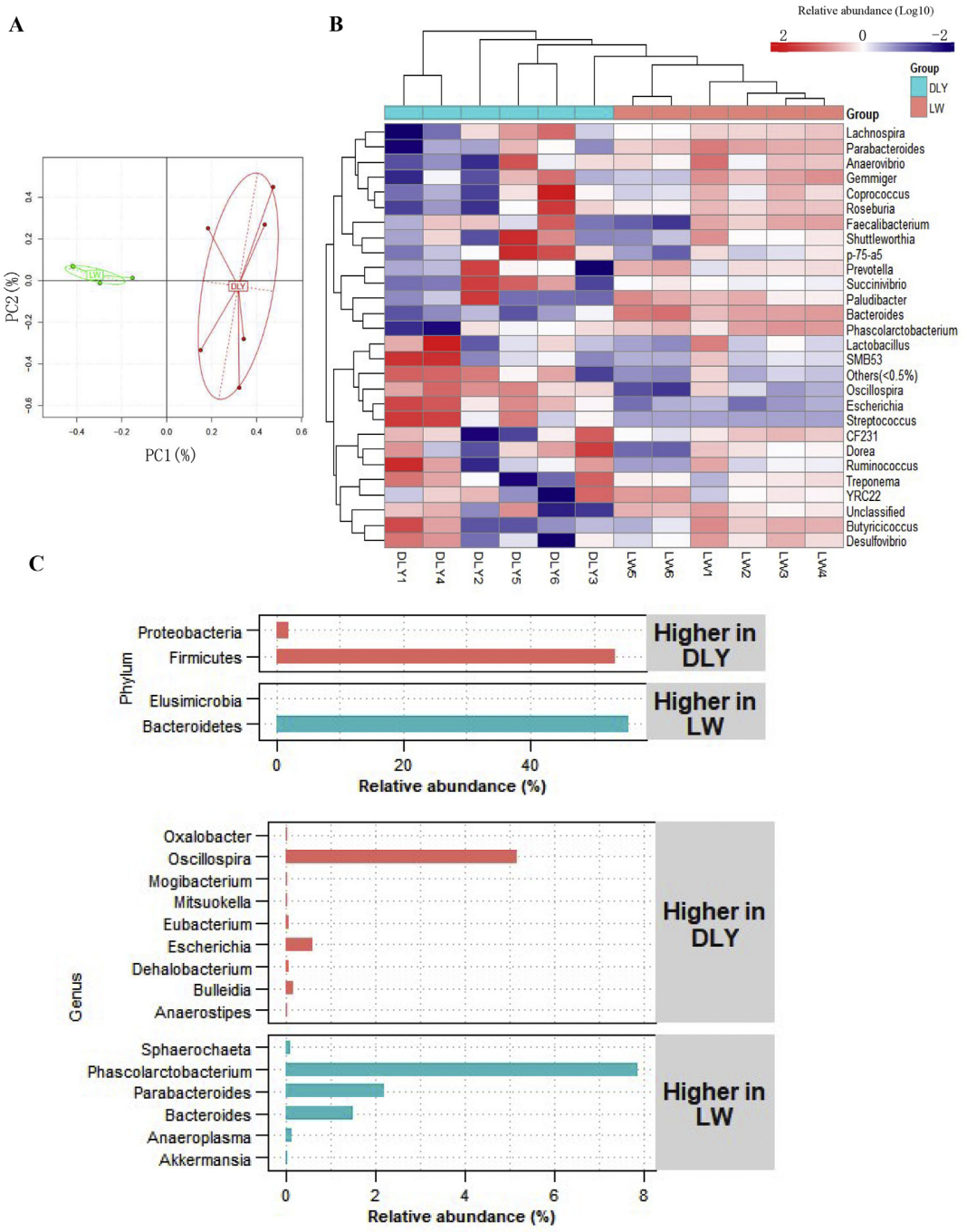

Fig. 1. Laiwu (LW) pigs harbor a distinct intestinal microbiota compared with crossbred (Duroc × [Landrace × Yorkshire]) DLY pigs. (A) PCA plot showing fecal microbiota compositional differences between LW pigs and DLY pigs. Each dot represents one pig. (B) Heatmap of cluster analysis of genera in the fecal microbial community between LW and DLY pigs. (C) Difference in microbial communities at phylum and genus level between LW and DLY pigs analyzed by metastats (the relative abundance > 1%).

distinct gut microbial composition of LW pigs from DLY pigs could be an efficient regulator in IMF deposition.

3.2. Fecal microbiota transplantation induced shifts on growth performance and diarrhea rate

The FMT assay was performed to further investigate the contribution of the microbial community to IMF deposition in pigs. Fecal microbiota suspensions from healthy LW pigs were passively transferred into the DLY pigs by oral administration (Fig. 2A). Considering the slow growth and low diarrhea rate of LW pigs, we also investigated the effects of FMT on growth performance and diarrhea rate. There was no significant difference ($P > 0.05$) in body weight during the whole experimental period (Fig. 2B). HFMT significantly increased ($P < 0.05$) feed conversion ratio but no difference was observed among the other three groups (Fig. 2C). In addition, a significantly decreased ($P < 0.05$) backfat thickness was also noticed in the HFMT group compared with control pigs (Fig. 2D). The reduction in backfat thickness of HFMT pigs might be correlated with the slow growth property of Chinese native pig breeds. Transplantation with a high dose of microbial suspension from LW pig into DLY pigs caused a similar decrease ($P < 0.001$) in

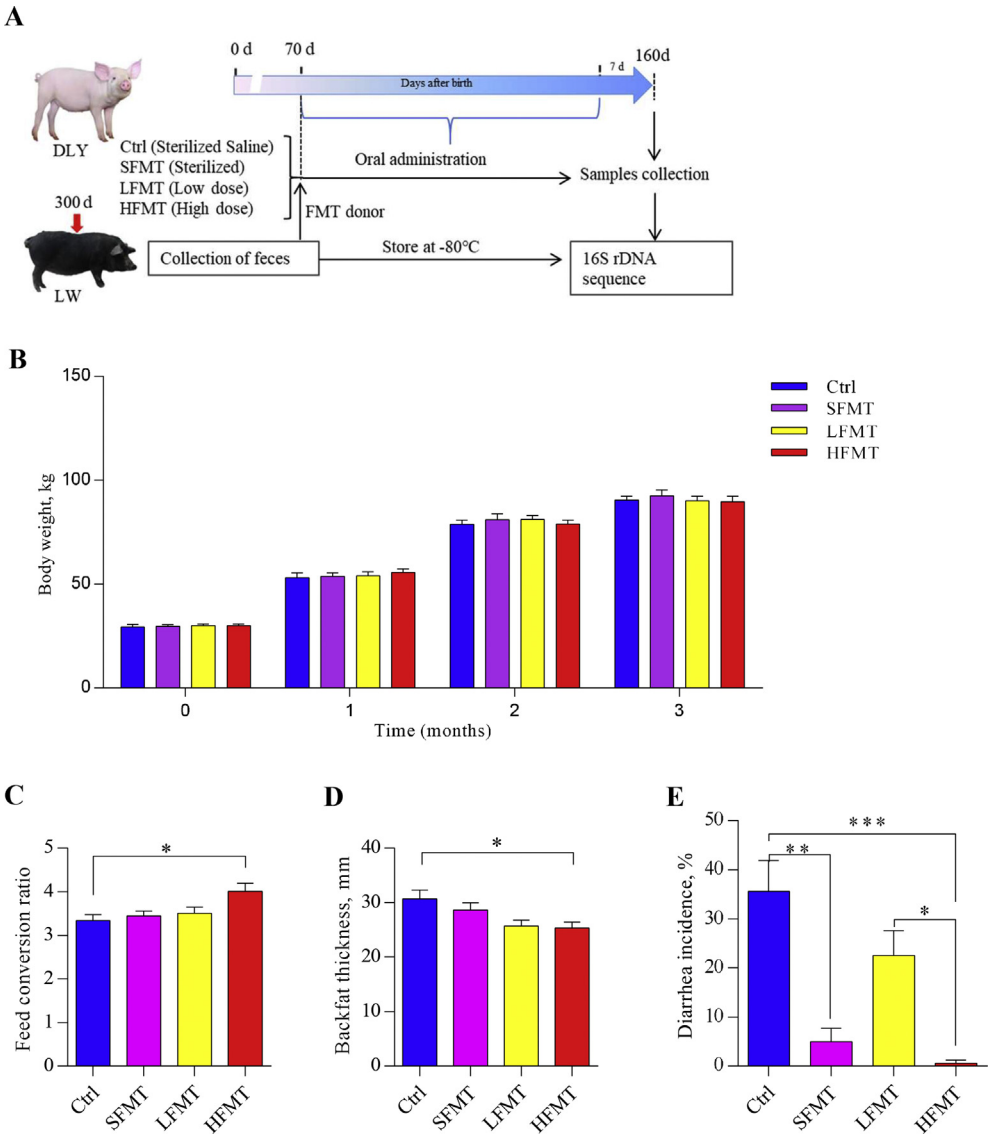

Fig. 2. Effect of fecal microbiota transplantation (FMT) on growth performance and diarrhea rate. (A) Experimental design. (B) Body weight was measured monthly. (C) Feed conversion ratio of pigs during experimental periods. (D) Backfat thickness. (E) The mean diarrhea incidences of pigs during d 0–30 after fecal microbiota transplantation. Error bars indicate SEM ($^{*}P < 0.05$, $^{**}P < 0.01$, $^{***}P < 0.001$) determined by one-way ANOVA. HFMT, high dose of fecal microbiota transplantation; LFMT, low dose of fecal microbiota transplantation; SFMT, sterile fecal microbiota transplantation.

diarrhea ratio (Fig. 2E), consistent with a previously published study that FMT from healthy native pig breeds into recipients significantly prevented stress-induced diarrhea (Hu et al., 2018). However, a significantly decreased ($P < 0.001$) diarrhea ratio was observed in SFMT pigs, whereas no reduction in diarrhea ratio in LFMT pigs was found compared with control pigs. So far, the exact functions of microorganisms and the risks of FMT are not yet fully understood. Due to the lack of strict and standardized screening for donor–acceptor in animal trials, FMT itself could turn out to be an infection factor (Gupta et al., 2021). Therefore, whether or not FMT ameliorated stress-induced diarrhea when a low concentration of fecal microbiota was administered, could not be demonstrated, as the SFMT pigs had less stress and did not show diarrhea.

3.3. Effect of FMT on meat quality

The results showed that significantly increased ($P < 0.05$) IMF percentage of longissimus dorsi in the HFMT group was observed compared with other groups (Fig. 3A). Further, HFMT significantly increased ($P < 0.05$) the value of L* and b* in longissimus dorsi compared with control pigs (Fig. 3B and D). L* value was higher ($P < 0.05$) in the LFMT group than that in the SFMT group (Fig. 3B). There was no significant difference ($P > 0.05$) in a* value among the 4 groups (Fig. 3C). However, other traits of pork including the marbling score, value of pH at 45 min and 24 h, protein percentage, drip loss and shear force of longissimus dorsi were not affected ($P > 0.05$) by FMT (Fig. 3E–J). These data revealed that FMT-mediated lipid deposition in longissimus dorsi is most efficient in high doses of FMT. Thus, we next concentrated on investigating the underlying mechanism of microbiota-induced IMF deposition in the HFMT group.

3.4. HFMT restored gut microbial composition

To directly investigate the impact of HFMT on the gut microbial composition of DLY pigs, the 16S rDNA gene of the microbiome was sequenced by Illumina MiSeq platform. The scatterplot based on

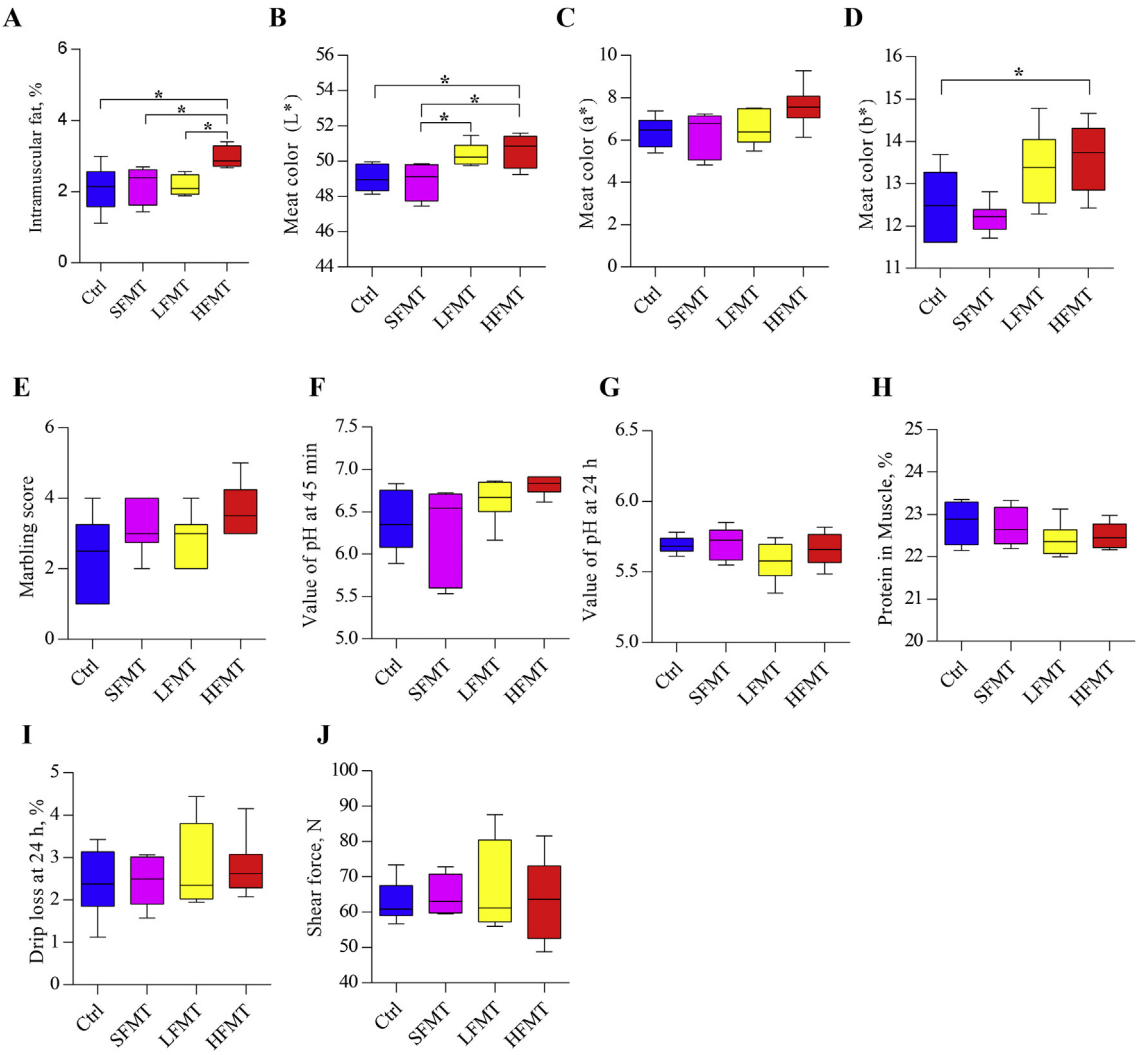

Fig. 3. Meat quality affected by fecal microbiota transplantation. (A) Intramuscular fat percentage of longissimus dorsi (%). Meat color of longissimus dorsi was measured by a Spectro colorimeter: (B) lightness (L*), (C) redness (a*), and (D) yellowness (b*). (E) Marbling score. (F and G) Value of pH at 45 min and 24 h. (H) Protein content in longissimus dorsi. (I) Drip loss at 24 h. (J) Share force. *$P < 0.05$, determined by one-way ANOVA.

principal coordinates analysis (PCoA) showed that the bacterial communities among groups were formed into 3 clusters and the cluster of samples in the HFMT group was between DLY and LW pigs (Fig. 4A). We observed that the microbial composition in HFMT and LW are closer to each other than to the Ctrl pigs based on the heatmap of UniFrac distance (Fig. 4B). In addition, the taxonomic analysis indicated that HFMT induced a shift from DLY pigs to LW pigs in the composition of fecal microbiota (Fig. 4C–G).

Analysis at the phylum level showed that fecal microbiota was dominated by four major phyla: Bacteroidetes, Firmicutes, Spirochaetes, and Proteobacteria. Compared to control pigs, HFMT administration was associated with a bloom of Bacteroidetes and reduction in Actinobacteria (Fig. 4C), whereas, the HFMT pigs had lower proportions of taxa on Firmicutes phylum, including class Clostridia, class Erysipelotrichia, order Clostridiales, order Erysipelotrichia, family Erysipelotrichaceae, genus *Blautia*, lower proportions of taxa on phylum Actinobacteria, including class Actinobacteria, order Coriobacteriales, family Coriobacteriaceae, and lower proportions of taxa on phylum Proteobacteria, including class Gammaproteobacteria, order Enterobacteriales, family Enterobacteriaceae. In contrast, HFMT induced higher proportions of Bacteroidetes, including class Bacteroidia, order Bacteroidales (Fig. 4C–G), which are reported to have desirable traits and the ability to metabolize complex carbohydrates and generate SCFA directly or via cross-feeding mechanisms (Ridaura et al., 2013). The significantly increased Bacteroides and decreased Firmicutes observed in HFMT pigs were closer to the property of microbial composition in LW pigs, indicating that FMT transferred the microbiota composition characteristics from LW pigs to DLY pigs.

3.5. HFMT affected small intestinal health and fecal SCFA concentration

A well-developed and mature intestinal physiology can improve intestinal function, regulate the uptake of energy by increasing gut transit time, maintain barrier function and mucosal integrity, and improve intestinal immunity (Hartenstein and Martinez, 2019; Stanghellini et al., 2016; Vanheel and Farre, 2013). To investigate whether HFMT contributes to the development and maturation of the small intestinal morphology in pigs, we performed H&E staining of the duodenum, jejunum, and ileum (Fig. 5A). The results indicated that the HFMT significantly increased ($P < 0.01$) villi heights in the duodenum, jejunum, and ileum (Fig. 5B) and decreased ($P < 0.05$)

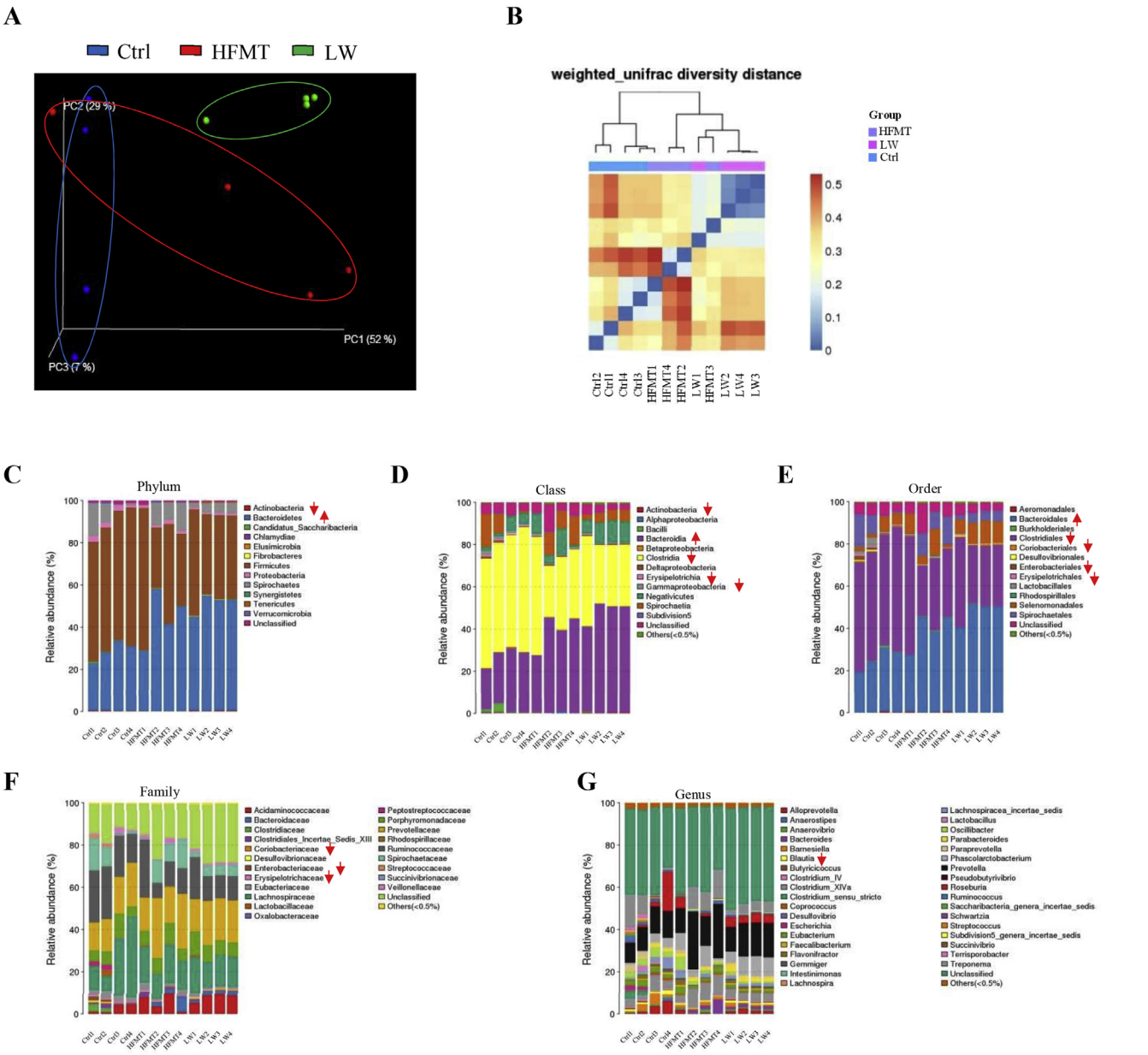

Fig. 4. Effect of fecal microbiota transplantation (HFMT) on fecal microbiota composition. (A) Scatterplot from PCoA in bacterial communities based on weighted UniFrac distance. (B) Heatmap showing the beta-diversity of bacterial community based on hierarchical clustering analysis of weighted UniFrac distances. Shifts in gut bacterial taxonomic compositions at several taxonomic levels after fecal microbiota transplantation, including (C) phylum, (D) class, (E) order, (F) family, and (G) genus. Upward and downward arrows show that the relative abundance of the corresponding taxonomic levels significantly increased and decreased with fecal microbiota transplantation, respectively.

crypts depths in the duodenum (Fig. 5C). Furthermore, a significant increase ($P < 0.05$) in the ratios of villi heights to crypts depths was observed from duodenum, jejunum, and ileum in HFMT pigs (Fig. 5D). These results suggested that HFMT promotes intestinal development and maintains intestinal villi integrity.

The complementary enzymes produced by gut microbiota depolymerize and ferment dietary polysaccharides into host absorbable SCFA (El Kaoutari et al., 2013). Specifically, SCFA have major impacts on host energy metabolism, such as providing substrates for lipogenesis (Turnbaugh et al., 2006). The shifts of gut microbial communities might cause changes in the production of microbial fermentation. Hence, we determined the concentration of acetic, propionic, isobutyric, butyric, isovaleric, and valeric acids in fecal samples using gas chromatography analysis. It is noteworthy that the concentration of isobutyric acid and isovaleric acid was significantly higher ($P < 0.05$) in HFMT pigs than that in control pigs. In addition, the HFMT pigs showed a tendency of a higher amount of acetic, propionic, butyric, and valeric acids (Fig. 5E). These data suggested that microbiota mediates the lipid deposition in muscle possibly by increasing the production of SCFA from intestinal fermentation.

3.6. HFMT induced muscle-specific metabolic profiling

Hypothesizing that intestinal microbiota was the critical mediator for IMF deposition, we sought to further determine the effects of microbiota transplantation on muscular lipidome. The untargeted lipidomic of longissimus dorsi was performed. Of the 7,109 ion features detected by LC–MS system, only 124 metabolites were

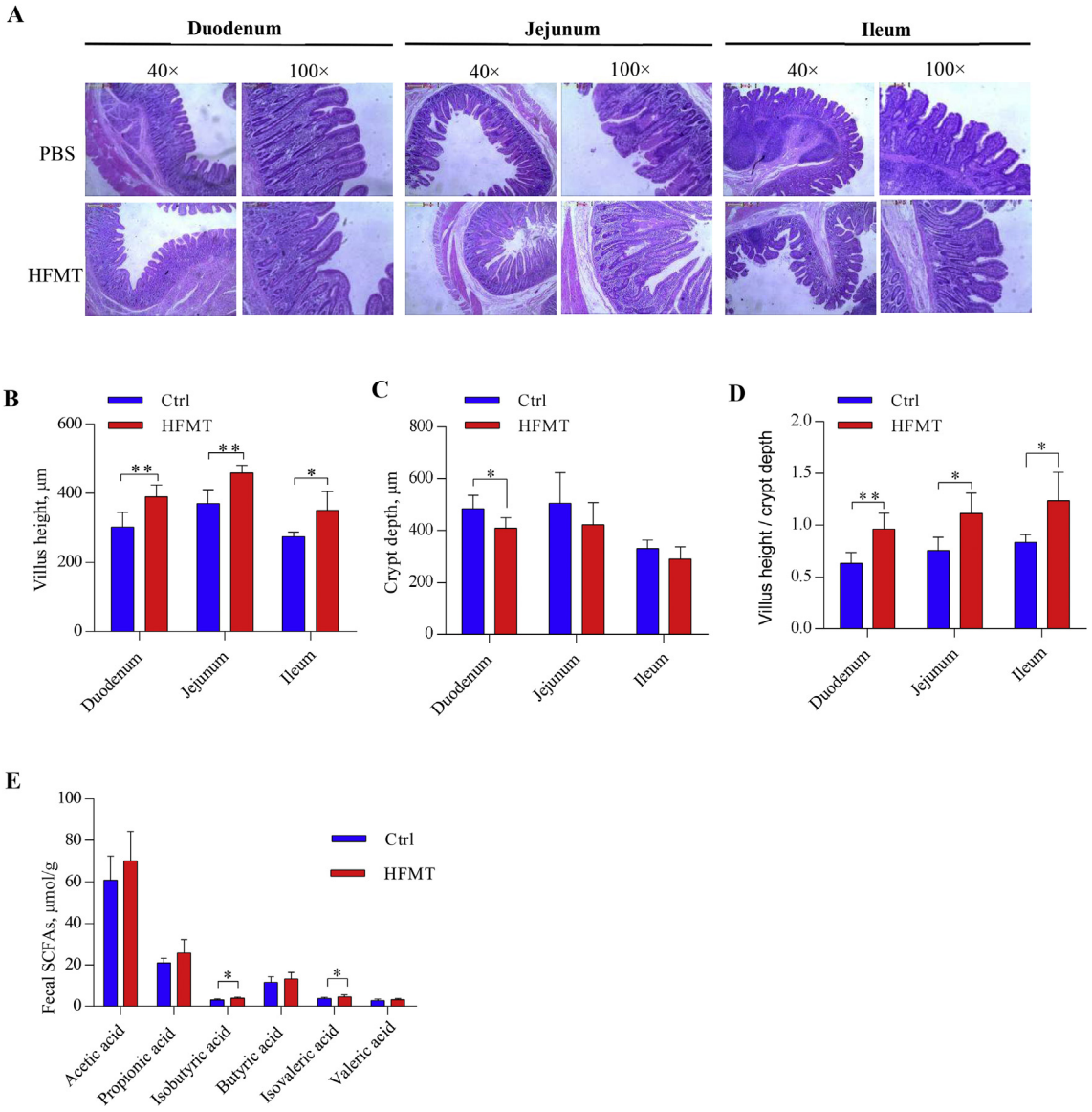

Fig. 5. The intestinal histological characteristic and fecal SCFA. (A) Representative H&E staining of intestine. The images of intestinal morphology are shown at 40× magnification and 100× magnification. (B–D) Statistical analysis of villus height, crypt depth, and the ratios of villus height to crypt depth in pigs. (E) Levels of fecal SCFA in HFMT and Ctrl groups. Data are shown as mean ± SEM (n = 5), using the unpaired Student's t-test (two-tailed), $^{*}P < 0.05$, $^{**}P < 0.01$. SCFA = short-chain fatty acids; HFMT = fecal microbiota transplantation.

identified to be considerably altered (VIP ≥ 1, fold change ≥ 1.2 or < 0.833, $P < 0.05$, respectively) after FMT. Principal coordinate analysis and heatmap of cluster analysis showed significant clustering of samples between control and HFMT (Fig. 6A and B). An altered abundance of metabolites suggested tissue physiology. For example, fatty acyls comprised 21.73% of muscular metabolites and made up only 11.4% altered by HFMT, while glycerophospholipids comprised 30.42% yet 47.37% were altered by HFMT (Fig. 6C and D). To characterize the correlations among the metabolites of different classes, we analyzed the correlations of altered metabolites in muscle. Comparative analysis of intra-tissue metabolite correlations indicated that glycerophospholipids had the strongest correlation with other metabolites (Fig. 6E).

3.7. HFMT induced changes in intestinal and muscular proteomic

The proteomic landscape of the small intestine and muscle, the key tissue for lipid absorption and deposition, was assessed by iTRAQ quantification project. Highly stringent criteria in raw data handling ensured the confident identification of 8,859 distinct peptides, corresponding overall to 2,037 unique proteins in muscle. In addition, 50,624 peptides and 7,866 proteins were identified in the small intestine. Using critical stringent criteria of fold change >1.5 or <0.5, $P < 0.05$, we identified 247 and 337 differentially expressed proteins in muscle and intestine, respectively. However, only 5 proteins were changed in both muscle and intestine (Fig. 7A).

To characterize the biological process and functions of the differentially expressed proteins in the intestine and muscle after FMT, the pathway analysis based on the KEGG database was performed. In the tissue of the intestine and muscle, the differential proteins affected by FMT were enriched in pathways including lipid metabolism, carbohydrate metabolism, and energy metabolism (Fig. 7B). We identified signaling pathways involved in lipid metabolism of HFMT small intestine and found that steroid hormone biosynthesis is significantly enriched in the top 40 KEGG pathways (Fig. 7C). In

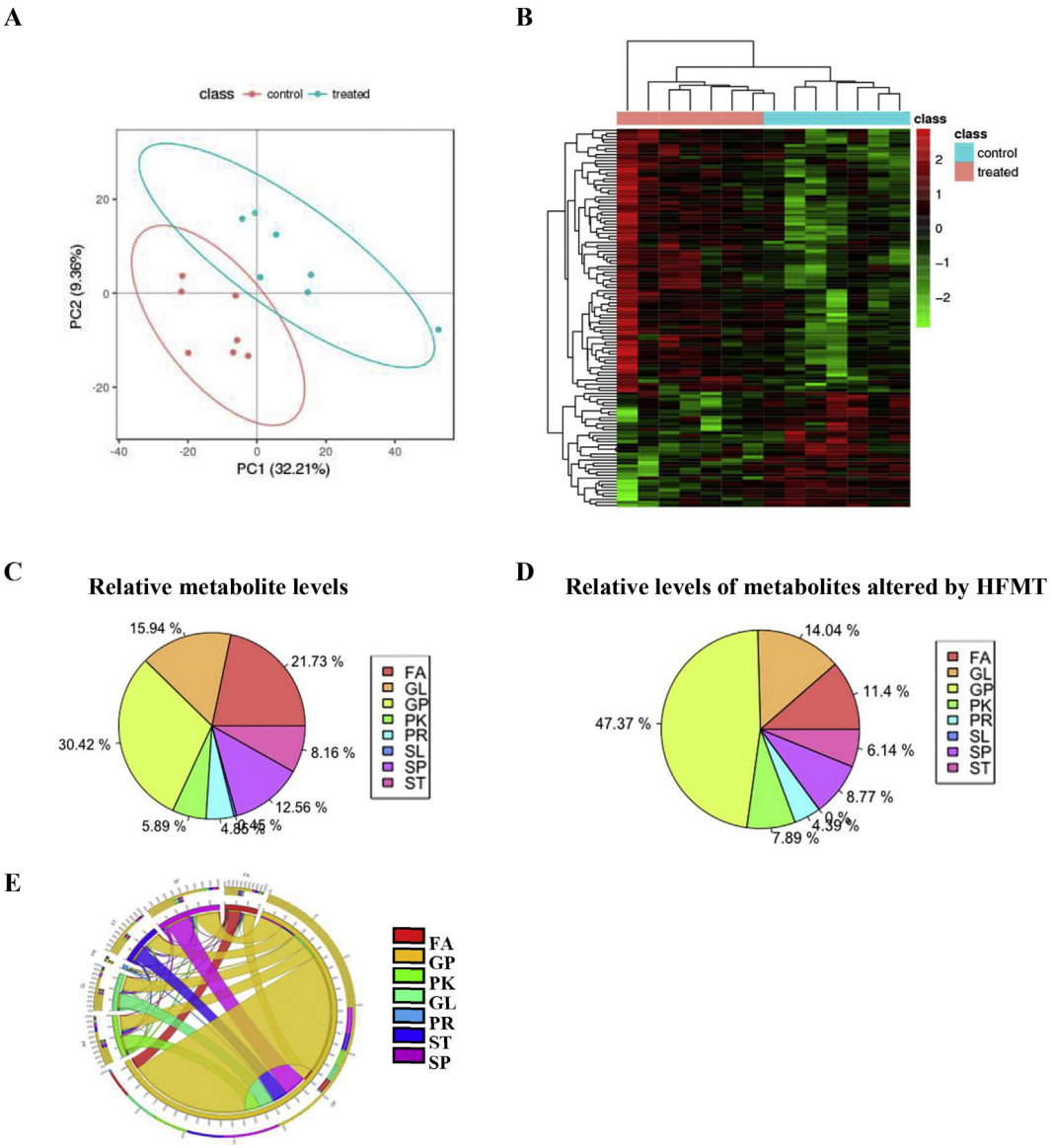

Fig. 6. Muscle-specific metabolic profiling. (A) Scatterplot from PCA. (B) Heatmap of metabolite clusters in muscle, measured by LC–MS based metabolomics. (C) Relative metabolite levels. (D) Relative levels of metabolites altered by HFMT. (E) Graphical visualization of significant correlations between the significantly altered metabolites of different class or within the same class. Each ribbon indicates a significant metabolites correlation between or within each metabolite class. Ribbon thickness refers to number of significantly correlated metabolites. Metabolites were ordered according to metabolite class as indicated in colored bar around the circumference. HFMT, high dose of fecal microbiota transplantation. FA = fatty acyls; GL = glycerolipids; GP = glycerophospholipids; PK = polyketides; PR = prenol lipids; SL = saccharolipids; SP = sphingolipids; ST = sterol lipids.

addition, the protein UniProt accessions and ratios of HFMT/Ctrl were uploaded into the Ingenuity Pathway Analysis (IPA) software in which the differentially regulated proteins were all characterized with statistical significance. Based on the network analysis using the IPA tool, we observed that the network "Lipid metabolism" was more highly enriched in HFMT group than Ctrl group (Fig. 7D and E).

To investigate the potential mechanisms of microbiota-mediated lipid deposition, the differentially expressed proteins associated with lipid metabolism are summarized in Table S6. The lipogenesis-associated biomarkers including fatty acid desaturase 1 (*FADS1*), fatty acid binding protein 4 (*FABP4*), and fatty acid synthase (*FASN*) were up-regulated in HFMT. Adenosine monophosphate-activated protein kinase (AMPK) which inhibits the expression of sterol-regulatory element-binding protein 1 (SREBP1) target lipogenic enzymes and reduces lipid accumulation (Shimano and Sato, 2017), was downregulated in HFMT pigs. In contrast, HFMT pigs had a decreased expression of proteins involved in fatty acid oxidation at mitochondrion, including acyl-CoA dehydrogenase medium chain (ACADM), acetyl-CoA acyltransferase 2 (ACAA2), and mitochondrial delta3, delta2-dienoyl-CoA isomerase (ECI1) (Table S6). Together, these results suggested that selective improvement of IMF might be through upregulating the expression of lipogenesis-associated genes.

3.8. Screening the core species-associated to IMF deposition

The linear discriminative features effect size (LEfSe) analysis (LDA > 2) was applied to identify specific bacterial taxa or species-level phylotypes that contribute to the IMF deposition and discover the taxonomic differences of specific bacteria in

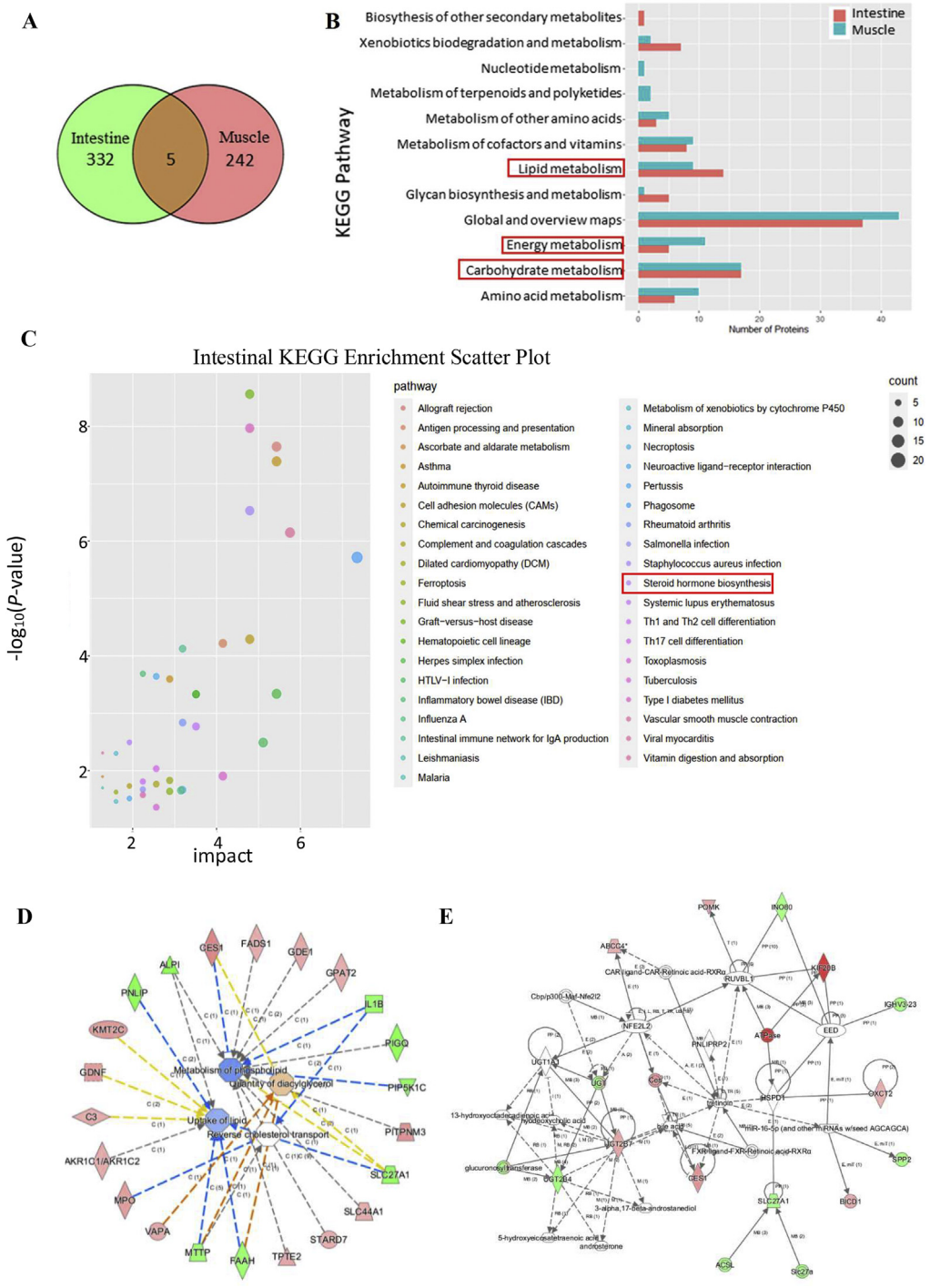

Fig. 7. The differentially expressed proteins and enriched pathways in the Intestine and Muscle of HFMT Pigs. (A) Venn diagram showing the number of HFMT-induced differentially expressed proteins in intestine and muscle. (B) KEGG pathway analysis of differentially proteins related to metabolic process. (C) Scatterplot for pathways in KEGG enrichment of differentially expressed proteins. The impact was calculated according to the number of annotated differentially proteins in this pathway term. (D and E) The network generated by Ingenuity Pathway Analysis (IPA) software shows enriched biological functions related to lipid metabolism (D), and the most enriched interaction network (E) of the differentially expressed proteins in HFMT-induced pigs. Red indicates up-regulated; green indicates down-regulated, white integrates proteins involved in certain network but not differentially expressed in this study. The degree of change for protein expression is indicated by color depth. HFMT, high dose of fecal microbiota transplantation. ABCC4 = multidrug resistance-associated protein 4; AKR1C1 = aldo-keto reductase family 1 member C1; ALPI = intestinal-type alkaline phosphatase; BICD1 = protein bicaudal D homolog 1; C3 = complement C3; CES1 = liver carboxylesterase 1; FAAH = fatty-acid amide hydrolase 1; FADS1 = fatty acid desaturase 1; GDE1 = glycerophosphodiester phosphodiesterase 1; GDNF = glial cell line-derived neurotrophic factor isoform 2; GPAT2 = glycerol-3-phosphate acyltransferase 2; IGHV3-23 = immunoglobulin heavy variable 3-23; IL1B = multifunctional fusion protein; INO80 = chromatin-remodeling ATPase INO80; KIF20B = kinesin-like protein KIF20B; KMT2C = histone-lysine N-methyltransferase 2C; MPO = myeloperoxidase; MTTP = microsomal triglyceride transfer protein large subunit; OXCT2 = succinyl-CoA:3-ketoacid coenzyme A transferase 2; PIGQ = phosphatidylinositol glycan anchor biosynthesis class Q; PIP5K1C = phosphatidylinositol 4-phosphate 5-kinase type-1 gamma; PITPNM3 = membrane-associated phosphatidylinositol transfer protein 3; PNLIP = pancreatic triacylglycerol lipase; POMK = protein-O-mannose kinase; SLC27A1 = solute carrier family 27 member 1; SLC44A1 = choline transporter-like protein 1; SPP2 = secreted phosphoprotein 24; STARD7 = StAR-related lipid transfer protein 7; TPTE2 = phosphatidylinositol 3 =4 =5-trisphosphate 3-phosphatase TPTE2; UGT = UDP-glucuronosyltransferase; VAPA = vesicle-associated membrane protein-associated protein A.

HFMT and LW pigs. The data revealed 50 discriminative features in LW pigs and 6 in the microbiota of HFMT pigs (Fig. 8A). This analysis also indicated that *P. piscolens* and *S. globose* were biomarker species in HFMT and LW pigs, respectively. In addition, we compared the relative abundance and found 5 bacterial species showed significantly higher abundance in HFMT pigs than that in control pigs. Of these, 4 bacterial species (*B. uniformis*, *S. globosa*, *H. saccharovorans*, and *P. piscolens*) exhibited a significantly higher relative abundance in LW pigs compared to control pigs (Fig. 8B–F). The relative abundance of these 4 species is shown in Table S7. Furthermore, the correlation analysis suggested that *H. saccharovorans*, and *P. piscolens* were

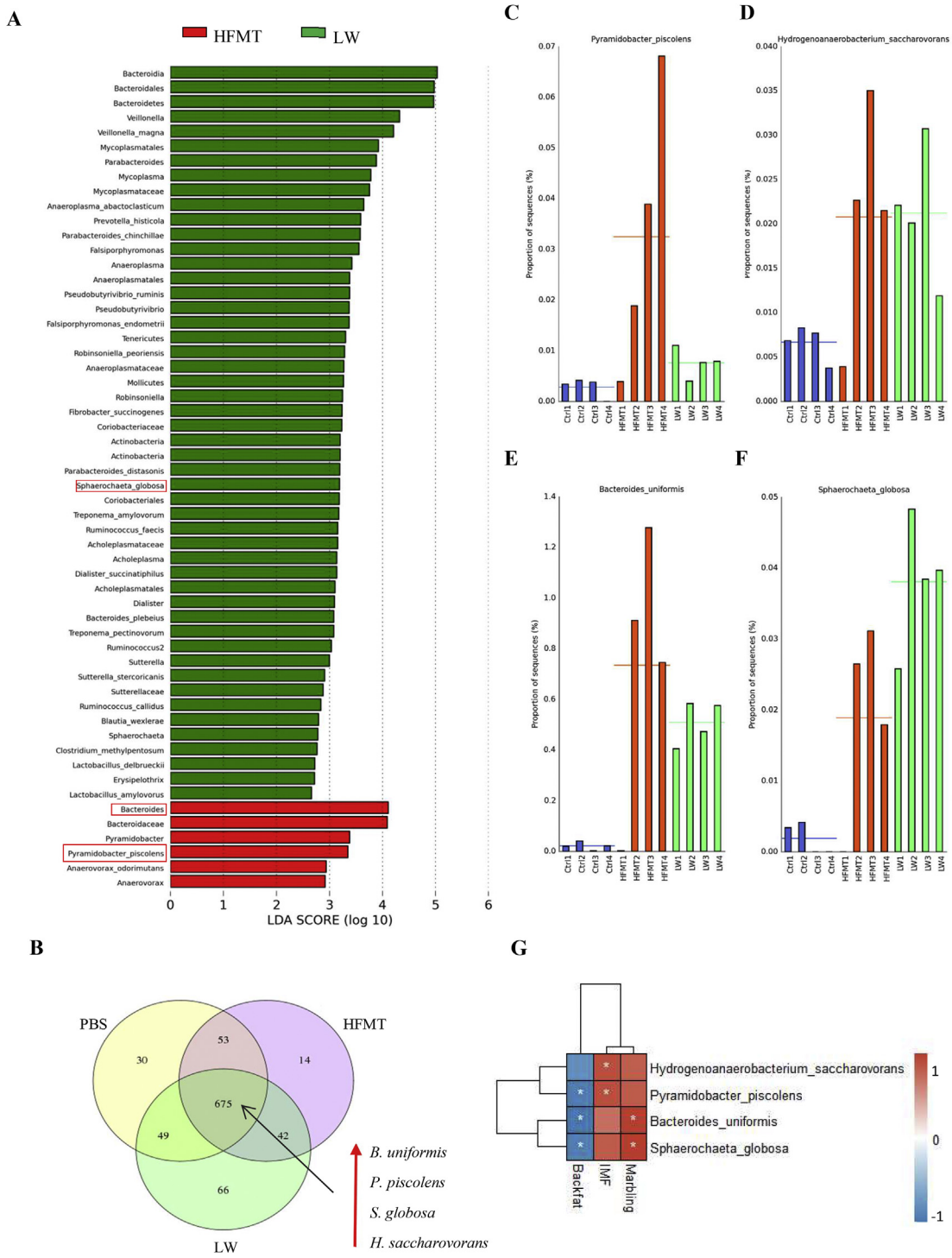

Fig. 8. Composite analysis to screen the core species-associated to IMF deposition. (A) The LEfSe analysis of intestinal bacterial communities. LEfSe analysis was performed by LEfSe software. (B) Venn diagrams of species. Upward arrows (red) showed that the relative abundances of microbial species were significantly increased by HFMT. (C to F) Bar plot of *Bacteroides_uniformis*, *Sphaerochaeta_globosa*, *Hydrogenoanaerobacterium_saccharovorans*, and *Pyramidobacter_piscolens* relative abundance, respectively. (G) Spearman correlation analysis between relative abundance of core bacterial species with fat deposition traits in HFMT pigs. *, Spearman correlation test $P < 0.05$. HFMT, high dose of fecal microbiota transplantation.

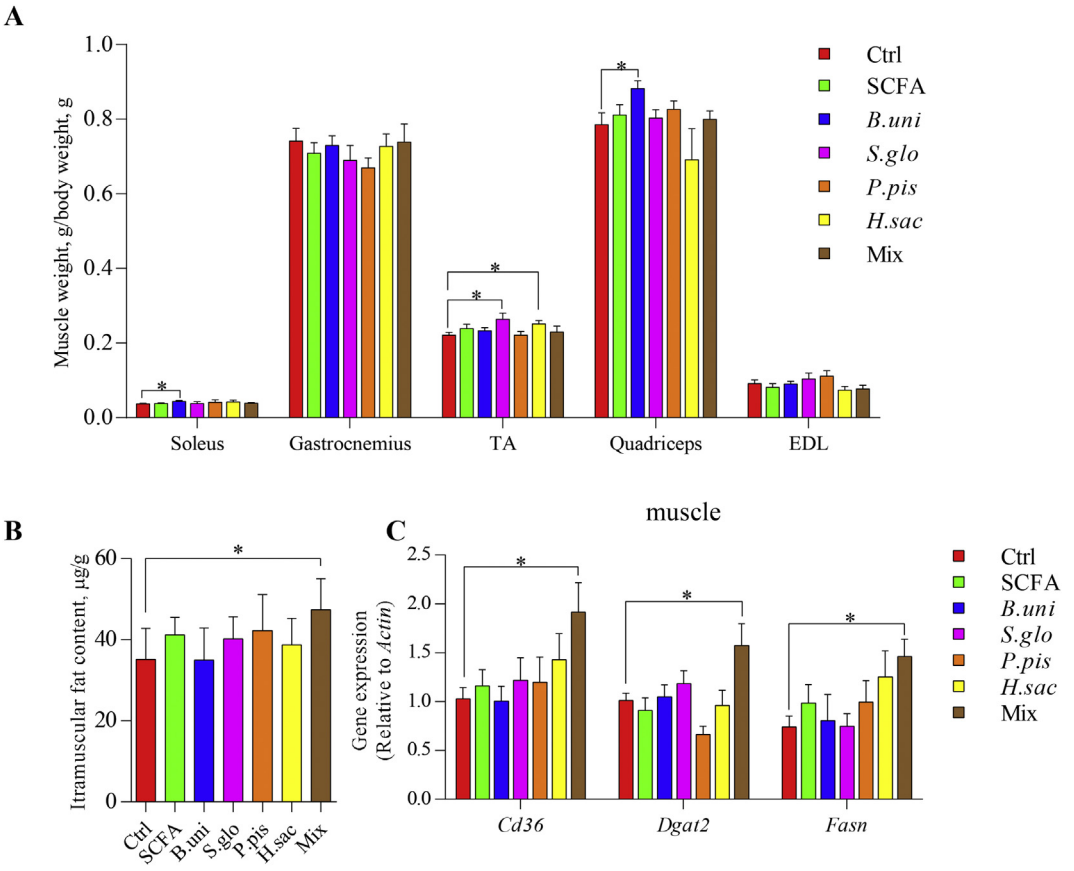

Fig. 9. Intestinal microbes administration changes fat deposition in mice. (A) Weights of soleus, gastrocnemius, tibialis anterior (TA), quadriceps, and extensor digitorum longus (EDL) muscles from mice ($n = 13$). (B) Intramuscular fat content in Quadriceps ($n = 5$). (C) *Cd36*, *Dgat2*, and *Fasn* mRNA expression levels in muscle, respectively. Data are expressed as means ± SEM. Data were analyzed using two-tailed unpaired Student *t*-test and were considered statistically significant at $^{*}P < 0.05$ between indicated groups. *Cd36* = cluster of differentiation 36; *Dgat2* = diacylglycerol O-acyltransferase 2; *Fasn* = fatty acid synthase. Ctrl, control; SCFA, mice were inoculated with short-chain fatty acid; *B.uni*, mice were inoculated with *Bcteroides uniformis*; *S.glo*, mice were inoculated with *Sphaerochaeta globosa*; *P.pis*, mice were inoculated with *Pyramidobacter piscolens*; *H.sac*, mice were inoculated with *Hydrogenoanaerobacterium saccharovorans*; Mix, mice were inoculated with the mixture of *B. uniformis*, *S. globosa*, *P. piscolens*, and *H. saccharovorans*.

positively correlated with IMF. *B. uniformis* and *S. globosa* were positively correlated with marbling and *B. uniformis*, *S. globosa*, and *P. piscolens* were negatively correlated with backfat thickness in HFMT pigs (Fig. 8G). Thus, these four bacterial species were considered as strong candidates that associate with the improvement of IMF in longissimus dorsi of pigs.

3.9. Oral administration of IMF deposition-associated microbes increased lipid accumulation in the muscle of mice

Next, we inoculated SPF C57BL/6j mice with the 4 bacteria (*B. uniformis*, *S. globosa*, *H. saccharovorans*, *P. piscolens*) alone or consortium by oral gavage every other day for 4 weeks. To ablate the microbiota, the mice were given an antibiotic cocktail supplement in drinking water for 1 week before the microbiota administration. SCFA generated by microbial fermentation of dietary polysaccharides were widely revolved in several microbiota-mediated effects on host lipid metabolism and obesity (Tremaroli and Backhed, 2012), and the increased levels of fecal SCFA were observed in this study. To investigate the causal relationship between the increased concentration of fecal SCFA and improvement of IMF in HFMT pigs, we set up a group that a mixture of SCFA was provided in the drinking water. Thus, the mice trial was performed to investigate and validate the mechanism of specific microbiota in IMF deposition.

After transplantation with microbes for 4 weeks, mice inoculated with bacteria consortium showed significantly higher ($P < 0.05$) IMF content in quadriceps (Fig. 9B), but there was no significant difference among other treatment mice. Mice inoculated with *B. uniformis* displayed an increase in ($P < 0.05$) soleus and quadriceps weight, and *S. globosa* and *H. saccharovorans* treated mice were increased ($P < 0.05$) in TA weight compared with control mice (Fig. 9A).

The AMPK mediated fat storage by regulating the expression of lipogenesis-association genes. Our proteomic data also indicated that the expression of AMPK was decreased, and lipogenesis-associated biomarkers were increased in HFMT pigs (Table S6). To further evaluate whether the mechanism of intestinal microbes-mediated lipid accumulation is involved in the AMPK pathway, the relative expression of genes associated with lipogenesis was measured by RT-PCR. As expected, elevated expression ($P < 0.05$) of *Cd36*, *Dgat2*, and *Fasn* was observed in the muscle of mixed bacteria recipient mice compared to control mice (Fig. 9C). Taken together, our data show that bacteria supplementation has profound effects on muscular fat deposition. The expression of lipogenesis-associated genes induced by selected bacteria supplementation,

thus, represents a new regulatory pathway by which microbes affect IMF deposition.

4. Discussion

Fecal microbiota transplantation, followed by integration analysis of metabolome, proteome, and microbiome, was used to investigate the host–microbiota interactions in meat quality, IMF content, intestinal morphology, and lipid metabolic function in pigs. Our study indicated that the inoculation of combined (*B. uniformis*, *S. globosa*, *H. saccharovorans*, and *P. piscolens*) microbes screened from gut microbiota can improve IMF deposition via upregulating the expression of lipogenesis-associated genes. Altogether, microbiota-mediation in the improvement of commercial pig production is summarized by: (1) improvement in IMF content and reduction of diarrhea rate, (2) alterations in the metabolism of small lipid molecules (fatty acyls, glycerolipids, and glycerophospholipids) in muscle, (3) enhancement of small intestine physiological functions (villi heights and the ratios of villi heights to crypts), and (4) upregulation of lipogenesis-associated genes in muscle.

To uncover the underlying mechanism of gut microbiota on lipid metabolism, we performed FMT and 16S rDNA sequencing. The data on intestinal taxonomic compositions at species level revealed that both *B. uniformis*, *S. globosa*, *H. saccharovorans*, and *P. piscolens* showed higher abundance in LW pigs and HFMT pigs than that in control pigs. These results suggested that *B. uniformis*, *S. globosa*, *H. saccharovorans*, and *P. piscolens* in the recipient pigs may consist of those strains harbored in recipient DLY pigs and those strains derived from donor feces. Moreover, the spearmen correlation analysis revealed that these 4 species were positively correlated with IMF and marbling, but negatively correlated with backfat thickness. It is known that species within Bacteroides exhibit remarkable diversity in polysaccharide utilization (Sonnenburg et al., 2010; Xu et al., 2007) and positive correlation with low-density lipoprotein (LDL), and high-density lipoprotein (HDL) cholesterol levels were found in a recent study with Japanese cedar pollinosis patients (Harata et al., 2017). In addition, commensal bacteria from phylum Bacteroidetes were critical for maintaining intestinal symbiosis and homeostasis via producing sphingolipids (Brown et al., 2019). The elevated levels of Bacteroidetes in HFMT pigs, as well as the consistent results from previous studies, suggest that the dominant Bacteroidetes may correlate with improvement of intestinal physiology and health in HFMT pigs. Nonetheless, limited data are available concerning the causality of FMT on the relationship between intestinal functions and IMF deposition, as well as the underlying mechanism, which remains to be further confirmed.

However, multiple studies have shown that obesity is associated with an altered microbial proportion characterized by depleted levels of Bacteroidetes and elevated levels of Firmicutes (Bervoets et al., 2013; Riva et al., 2017; Xu et al., 2012). The increased ratio of Firmicutes to Bacteroidetes may be associated with increased capacity for energy harvest from colon fermentation and contribute to the pathophysiology of obesity (Fernandes et al., 2014; Turnbaugh et al., 2006). Other evidence indicated that *B. uniformis* was more abundant in lean women (Dugas et al., 2018), and ameliorated lipid metabolic dysfunction in high-fat diet induced obesity (Gauffin Cano et al., 2012). Here, the 16S rDNA sequencing indicated that the most abundant phylum in feces of HFMT pigs and LW pigs were Bacteroidetes which shown a significantly higher relative proportion in LW pigs than that in DLY pigs. In addition, the HFMT pigs harbored a significantly higher abundance of *B. uniformis*. We, therefore, speculate that the high abundance of phylum Bacteroidetes and species *B. uniformis* may relate to decreased backfat thickness in HFMT pigs. Earlier studies also indicated that manipulation of dietary composition can selectively increase IMF percentage without impact on subcutaneous backfat deposition (Doran et al., 2006; Wood et al., 2004). Consistent with previous studies, our evidence supports the view that genetic correlation between IMF and backfat is not always strong and that is possible to regulate them independently by microbiota or dietary manipulation.

We did not observe a significant change in the fat deposition but showed an effect on increasing muscle weight after *B. uniformis* inoculation of mice. Besides, increased IMF content and high expression of lipogenesis-associated genes were observed only in mice inoculated with consortium microbes. Thus, the *B. uniformis* may promote muscle development, and compound microorganisms can selectively improve IMF deposition. Notably, HFMT pigs produced a higher amount of fecal SCFA compared with control pigs. However, there were no significant differences in IMF and muscular weight in SCFA treatment mice. Therefore, the effects of gut microbiota on IMF deposition were not via production of SCFA.

Gut microbiota and the microbial metabolites in mammals play a crucial role in lipid metabolism and fat storage (Martinez-Guryn et al., 2018; Suarez-Zamorano et al., 2015). The mechanism by which the gut microbiota influences lipid metabolism may involve the AMPK pathway. Inhibition of AMPK activity results in an increase in nuclear translocation of the SREBP1 (Porstmann et al., 2008), which regulates gene expression of lipogenic enzymes (*FASN*, *ACACA*, *ELOVL6*, *SCD*). Moreover, the expression of AMPK has a direct effect on lipid synthesis by hydroxymethylglutaryl-CoA reductase and acetyl-CoA carboxylase (ACC1) (Gwinn et al., 2008). In this study, proteomic analysis revealed that the gut microbiota suppresses skeletal muscle expression of AMPK (Table S6), promotes expression of FASN (Fig. 9C), and thereby improves fat storage in muscle. In addition, studies indicated that CD36 is a key protein involved in facilitating the transport of fatty acids into myocytes (Bonen et al., 2004a). The increase in sarcolemma CD36 content correlated well with rates of fatty acid transport in muscle (Bonen et al., 2004b). Consistent with these studies, we identified an increased expression of *Cd36* gene in consortium microbes treated mice, suggesting that an altered abundance of members in these species contribute to the translation and deposition of muscular fat.

5. Conclusion

In summary, our data demonstrated that gut-specific microbial communities are efficient in promoting lipid accumulation in skeletal muscle, and this effect is at least, in part, mediated by the expression of AMPK and lipogenesis-associated genes. Our results indicated that the microbiome of Chinese indigenous pigs has an increased capacity for IMF deposition and this trait can be transferred via FMT. Thus, precision discrimination and administration of the functional microorganisms may be a potential strategy to modulate IMF and subcutaneous fat individually. In the context of the reduction in meat quality and IMF content of the livestock industry, our study showed that the manipulation of gut microbiota can promote muscular fat deposition in pigs and mice, implying that the gut microbiome is an efficient mediator improving the IMF content and meat quality, with a large potential application.

Author contributions

Chunlin Xie: Conceptualization, Methodology, Validation, Formal analysis, Investigation, Visualization, Writing - Original Draft; **Junyong Teng**: Investigation, Validation, Formal analysis; **Xinkai Wang**: Investigation, Validation; **Baoyang Xu**: Investigation, Visualization; **Yaorong Niu**: Investigation, Validation; **Libao**

Ma: Supervision, Resources; **Xianghua Yan**: Conceptualization, Supervision, Project administration, Funding acquisition.

Declaration of competing interest

We declare that we have no financial and personal relationships with other people or organizations that can inappropriately influence our work, and there is no professional or other personal interest of any nature or kind in any product, service and/or company that could be construed as influencing the content of this paper.

Acknowledgments

This work was supported by the National Key Research and Development Project (2018YFD0500404), the Natural Science Foundation of China (31730090, 31925037), and Hubei Provincial Natural Science Foundation of China (2018CFA020).

Appendix Supplementary data

Supplementary data to this article can be found online at https://doi.org/10.1016/j.aninu.2021.10.010.

References

Bervoets L, Van Hoorenbeeck K, Kortleven I, Van Noten C, Hens N, Vael C, et al. Differences in gut microbiota composition between obese and lean children: a cross-sectional study. Gut Pathog 2013;5:10.
Bonen A, Campbell SE, Benton CR, Chabowski A, Coort SLM, Han XX, et al. Regulation of fatty acid transport by fatty acid translocase/CD36. Proc Nutr Soc 2004a;63:245–9.
Bonen A, Parolin ML, Steinberg GR, Calles-Escandon J, Tandon NN, Glatz JFC, et al. Triacylglycerol accumulation in human obesity and type 2 diabetes is associated with increased rates of skeletal muscle fatty acid transport and increased sarcolemmal FAT/CD36. Faseb J 2004b;18:1144–6.
Brown EM, Ke X, Hitchcock D, Jeanfavre S, Avila-Pacheco J, Nakata T, et al. Bacteroides-derived sphingolipids are critical for maintaining intestinal homeostasis and symbiosis. Cell Host Microbe 2019;25:668–80. e667.
Chen W, Fang G, Wang S, Wang H, Zeng Y. Longissimus lumborum muscle transcriptome analysis of Laiwu and Yorkshire pigs differing in intramuscular fat content. Genes Genomics 2017;39:759–66.
Chevalier C, Stojanovic O, Colin DJ, Suarez-Zamorano N, Tarallo V, Veyrat-Durebex C, et al. Gut microbiota orchestrates energy homeostasis during cold. Cell 2015;163:1360–74.
Choi JS, Lee HJ, Jin SK, Choi YI, Lee JJ. Comparison of carcass characteristics and meat quality between duroc and crossbred pigs. Korean J Food Sci Anim Resour 2014;34:238–44.
Claesson MJ, Jeffery IB, Conde S, Power SE, O'Connor EM, Cusack S, et al. Gut microbiota composition correlates with diet and health in the elderly. Nature 2012;488:178–84.
Crespo-Piazuelo D, Criado-Mesas L, Revilla M, Castello A, Noguera JL, Fernandez AI, et al. Identification of strong candidate genes for backfat and intramuscular fatty acid composition in three crosses based on the Iberian pig. Sci Rep 2020;10:13962.
Desai MS, Seekatz AM, Koropatkin NM, Kamada N, Hickey CA, Wolter M, et al. A dietary fiber-deprived gut microbiota degrades the colonic mucus barrier and enhances pathogen susceptibility. Cell 2016;167:1339–53. e1321.
Doran O, Moule SK, Teye GA, Whittington FM, Hallett KG, Wood JD. A reduced protein diet induces stearoyl-CoA desaturase protein expression in pig muscle but not in subcutaneous adipose tissue: relationship with intramuscular lipid formation. Br J Nutr 2006;95:609–17.
Dugas LR, Bernabe BP, Priyadarshini M, Fei N, Park SJ, Brown L, et al. Decreased microbial co-occurrence network stability and SCFA receptor level correlates with obesity in African-origin women. Sci Rep 2018;8:17135.
Dunn WB, Broadhurst D, Begley P, Zelena E, Francis-McIntyre S, Anderson N, et al. Procedures for large-scale metabolic profiling of serum and plasma using gas chromatography and liquid chromatography coupled to mass spectrometry. Nat Protoc 2011;6:1060–83.
Dyar KA, Lutter D, Artati A, Ceglia NJ, Liu Y, Armenta D, et al. Atlas of circadian metabolism reveals system-wide coordination and communication between clocks. Cell 2018;174:1571–85. e1511.
El Kaoutari A, Armougom F, Gordon JI, Raoult D, Henrissat B. The abundance and variety of carbohydrate-active enzymes in the human gut microbiota. Nat Rev Microbiol 2013;11:497–504.
Fabbiano S, Suarez-Zamorano N, Chevalier C, Lazarevic V, Kieser S, Rigo D, et al. Functional gut microbiota remodeling contributes to the caloric restriction-induced metabolic improvements. Cell Metab 2018;28:907–21. e907.
Fassarella M, Blaak EE, Penders J, Nauta A, Smidt H, Zoetendal EG. Gut microbiome stability and resilience: elucidating the response to perturbations in order to modulate gut health. Gut 2020:1–11.
Fernandes J, Su W, Rahat-Rozenbloom S, Wolever TM, Comelli EM. Adiposity, gut microbiota and faecal short chain fatty acids are linked in adult humans. Nutr Diabetes 2014;4:e121.
Franzosa EA, Sirota-Madi A, Avila-Pacheco J, Fornelos N, Haiser HJ, Reinker S, et al. Gut microbiome structure and metabolic activity in inflammatory bowel disease. Nat Microbiol 2019;4:293–305.
Gauffin Cano P, Santacruz A, Moya A, Sanz Y. Bacteroides uniformis CECT 7771 ameliorates metabolic and immunological dysfunction in mice with high-fat-diet induced obesity. PLoS One 2012;7:e41079.
Godfray HCJ, Aveyard P, Garnett T, Hall JW, Key TJ, Lorimer J, et al. Meat consumption, health, and the environment. Science 2018;361:243–50.
Gupta S, Mullish BH, Allegretti JR. Fecal microbiota transplantation: the evolving risk landscape. Am J Gastroenterol 2021;116:647–56.
Gwinn DM, Shackelford DB, Egan DF, Mihaylova MM, Mery A, Vasquez DS, et al. AMPK phosphorylation of raptor mediates a metabolic checkpoint. Mol Cell 2008;30:214–26.
Hamilton MJ, Weingarden AR, Sadowsky MJ, Khoruts A. Standardized frozen preparation for transplantation of fecal microbiota for recurrent clostridium difficile infection. Am J Gastroenterol 2012;107:761–7.
Harata G, Kumar H, He F, Miyazawa K, Yoda K, Kawase M, et al. Probiotics modulate gut microbiota and health status in Japanese cedar pollinosis patients during the pollen season. Eur J Nutr 2017;56:2245–53.
Hartenstein V, Martinez P. Structure, development and evolution of the digestive system. Cell Tissue Res 2019;377:289–92.
Hu J, Ma L, Nie Y, Chen J, Zheng W, Wang X, et al. A microbiota-derived bacteriocin targets the host to confer diarrhea resistance in early-weaned piglets. Cell Host Microbe 2018;24:817–32. e818.
Hu J, Nie Y, Chen J, Zhang Y, Wang Z, Fan Q, et al. Gradual changes of gut microbiota in weaned miniature piglets. Front Microbiol 2016;7:1727.
Huang W, Zhang X, Li A, Xie L, Miao X. Genome-wide analysis of mrnas and lncrnas of intramuscular fat related to lipid metabolism in two pig breeds. Cell Physiol Biochem 2018;50:2406–22.
Kyriakis SC, Tsiloyiannis VK, Vlemmas J, Sarris K, Tsinas AC, Alexopoulos C, et al. The effect of probiotic LSP 122 on the control of post-weaning diarrhoea syndrome of piglets. Res Vet Sci 1999;67:223–8.
Lahiri S, Kim H, Garcia-Perez I, Reza MM, Martin KA, Kundu P, et al. The gut microbiota influences skeletal muscle mass and function in mice. Sci Transl Med 2019;11.
Lambe NR, Clelland N, Draper J, Smith EM, Yates J, Bunger L. Prediction of intramuscular fat in lamb by visible and near-infrared spectroscopy in an abattoir environment. Meat Sci 2021;171:108286.
Ley RE, Backhed F, Turnbaugh P, Lozupone CA, Knight RD, Gordon JI. Obesity alters gut microbial ecology. Proc Natl Acad Sci USA 2005;102:11070–5.
Ley RE, Turnbaugh PJ, Klein S, Gordon JI. Microbial ecology - human gut microbes associated with obesity. Nature 2006;444:1022–3.
Li G, Xie C, Lu S, Nichols RG, Tian Y, Li L, et al. Intermittent fasting promotes white adipose browning and decreases obesity by shaping the gut microbiota. Cell Metab 2017;26:672–85. e674.
Li H, Xu H, Li Y, Jiang Y, Hu Y, Liu T, et al. Alterations of gut microbiota contribute to the progression of unruptured intracranial aneurysms. Nat Commun 2020a;11:3218.
Li Z, Gao X, Peng X, May Chen MJ, Li Z, Wei B, et al. Multi-omics characterization of molecular features of gastric cancer correlated with response to neoadjuvant chemotherapy. Sci Adv 2020b;6:eaay4211.
Liu BH, Yuan JY, Yiu SM, Li ZY, Xie YL, Chen YX, et al. COPE: an accurate k-mer-based pair-end reads connection tool to facilitate genome assembly. Bioinformatics 2012;28:2870–4.
Lonergan SM, Huff-Lonergan E, Rowe LJ, Kuhlers DL, Jungst SB. Selection for lean growth efficiency in Duroc pigs influences pork quality. J Anim Sci 2001;79:2075–85.
Mars RAT, Yang Y, Ward T, Houtti M, Priya S, Lekatz HR, et al. Longitudinal multi-omics reveals subset-specific mechanisms underlying irritable bowel syndrome. Cell 2020;182:1460–73. e1417.
Martinez-Guryn K, Hubert N, Frazier K, Urlass S, Musch MW, Ojeda P, et al. Small intestine microbiota regulate host digestive and absorptive adaptive responses to dietary lipids. Cell Host Microbe 2018;23:458–69. e455.
Porstmann T, Santos CR, Griffiths B, Cully M, Wu M, Leevers S, et al. SREBP activity is regulated by mTORC1 and contributes to Akt-dependent cell growth. Cell Metab 2008;8:224–36.
Ridaura VK, Faith JJ, Rey FE, Cheng JY, Duncan AE, Kau AL, et al. Gut microbiota from twins discordant for obesity modulate metabolism in mice. Science 2013;341:1079-U1049.
Riva A, Borgo F, Lassandro C, Verduci E, Morace G, Borghi E, et al. Pediatric obesity is associated with an altered gut microbiota and discordant shifts in Firmicutes populations. Environ Microbiol 2017;19:95–105.
Rusc A, Sieczkowska H, Krzecio E, Antosik K, Zybert A, Kocwin-Podsiadla M, et al. The association between acyl-CoA synthetase (ACSL4) polymorphism and

intramuscular fat content in (Landrace x Yorkshire) x Duroc pigs. Meat Sci 2011;89:440–3.
Salma U, Miah AG, Maki T, Nishimura M, Tsujii H. Effect of dietary Rhodobacter capsulatus on cholesterol concentration and fatty acid composition in broiler meat. Poult Sci 2007;86:1920–6.
Savitski MM, Wilhelm M, Hahne H, Kuster B, Bantscheff M. A scalable approach for protein false discovery rate estimation in large proteomic data sets. Mol Cell Proteomics 2015;14:2394–404.
Shimano H, Sato R. SREBP-regulated lipid metabolism: convergent physiology - divergent pathophysiology. Nat Rev Endocrinol 2017;13:710–30.
Sonnenburg ED, Zheng HJ, Joglekar P, Higginbottom SK, Firbank SJ, Bolam DN, et al. Specificity of polysaccharide use in intestinal bacteroides species determines diet-induced microbiota alterations. Cell 2010;141:1241–52.
Stanghellini V, Chan FK, Hasler WL, Malagelada JR, Suzuki H, Tack J, et al. Gastroduodenal disorders. Gastroenterology 2016;150:1380–92.
Suarez-Belloch J, Guada JA, Latorre MA. Effects of sex and dietary lysine on performances and serum and meat traits in finisher pigs. Animal 2015;9:1731–9.
Suarez-Zamorano N, Fabbiano S, Chevalier C, Stojanovic O, Colin DJ, Stevanovic A, et al. Microbiota depletion promotes browning of white adipose tissue and reduces obesity. Nat Med 2015;21:1497–501.
Tremaroli V, Backhed F. Functional interactions between the gut microbiota and host metabolism. Nature 2012;489:242–9.
Turnbaugh PJ, Ley RE, Mahowald MA, Magrini V, Mardis ER, Gordon JI. An obesity-associated gut microbiome with increased capacity for energy harvest. Nature 2006;444:1027–31.
Vanheel H, Farre R. Changes in gastrointestinal tract function and structure in functional dyspepsia. Nat Rev Gastroenterol Hepatol 2013;10:142–9.
Wen B, Zhou R, Feng Q, Wang QH, Wang J, Liu SQ. IQuant: an automated pipeline for quantitative proteomics based upon isobaric tags. Proteomics 2014;14:2280–5.
Wood JD, Enser M, Fisher AV, Nute GR, Sheard PR, Richardson RI, et al. Fat deposition, fatty acid composition and meat quality: a review. Meat Sci 2008;78:343–58.
Wood JD, Nute GR, Richardson RI, Whittington FM, Southwood O, Plastow G, et al. Effects of breed, diet and muscle on fat deposition and eating quality in pigs. Meat Sci 2004;67:651–67.
Wu T, Zhang Z, Yuan Z, Lo LJ, Chen J, Wang Y, et al. Distinctive genes determine different intramuscular fat and muscle fiber ratios of the longissimus dorsi muscles in Jinhua and landrace pigs. PLoS One 2013;8:e53181.
Xu J, Mahowald MA, Ley RE, Lozupone CA, Hamady M, Martens EC, et al. Evolution of symbiotic bacteria in the distal human intestine. PLoS Biol 2007;5:1574–86.
Xu PR, Li M, Zhang JH, Zhang T. Correlation of intestinal microbiota with overweight and obesity in Kazakh school children. BMC Microbiol 2012;12.
Yang X, Zhang B, Guo Y, Jiao P, Long F. Effects of dietary lipids and Clostridium butyricum on fat deposition and meat quality of broiler chickens. Poult Sci 2010;89:254–60.
Zhernakova A, Kurilshikov A, Bonder MJ, Tigchelaar EF, Schirmer M, Vatanen T, et al. Population-based metagenomics analysis reveals markers for gut microbiome composition and diversity. Science 2016;352:565–9.